Centralized Cooperative Directional Spectrum Sensing for Cognitive Radio Networks

Woongsoo Na, Jongha Yoon, Sungrae Cho, David Griffith, and Nada Golmie

***Abstract*—Most previous spectrum sensing techniques use omni-directional antennas. Unlike omni-directional antennas, the use of directional antennas for spectrum sensing is a promising technique that can realize fine-grained sensing for the primary user (PU) with a longer sensing range. In this paper, we propose a centralized cooperative directional sensing technique for cognitive radio networks. We assume that one secondary coordinator called the fusion center (FC), gathers sensing results from secondary nodes. Using the reported information, the FC optimizes the sensing period, sensing power, and sensing beams per secondary node. For optimization, we use a modified gradient descent method with numerical methods to solve the nonlinear optimization problem. The simulation results show that our directional spectrum sensing technique is well suited for the existing cognitive radio environment. The optimal scheme shows proposed here better performance in all simulation factors than the non-optimized scheme.**

***Index Terms*—directional sensing, cognitive radio, spectrum sensing, optimization, and gradient decent**

I. Introduction

ONE of the core technologies used in cognitive radios is spectrum sensing to identify the availability of the spectrum for improving utilization. In cognitive radio networks (CRNs), secondary users (SUs) perform spectrum sensing to detect chunks of unused spectrum licensed to primary users (PUs) [7]. After detection, they deploy a secondary CRN in the available spectrum. Sensing may be performed regularly or occasionally to verify if the channel is vacant and/or to verify that the channel quality is acceptable. If one of these conditions is violated, the CR node decides either to change its configuration (e.g., transmission power) to decrease the interference level and compensate for the channel effects, or to switch to a new vacant channel. However, SUs do not always provide perfect sensing results, i.e., an SU may determine that the sensed spectrum is occupied by a PU when the spectrum is actually free *(false alarm)* or that the spectrum is free when a PU is actually present in the sensed channel *(miss detection)*. Many factors such as multipath fading, shadowing, and the receiver uncertainty problem1 may result in the above problems[1] may result in the above problems [4]. In order to overcome these problems, SUs can cooperate and share their sensing results with other SUs *(cooperative sensing)*. The spatially collected sensing results help determine whether the detected spectrum is actually vacant [4].

Cooperative sensing techniques for CRNs have been for many years. These techniques are classified into two categories: (1) *centralized* and (2) *distributed* [4]. In centralized techniques [5], [11], [13], [34], [36], [40], [44], there is a fusion center (FC) collects the sensing information from SUs. After gathering the sensing information, the FC computes the sensing schedule for a channel of each SU and disseminates a sensing task to the SUs. In the distributed approach [8], [10], [14], [19], [27], [32], [37], [42], [45], the SUs share sensing information among themselves and determine sensing parameters based on collected neighboring sensing information.

Most previous cooperative spectrum sensing techniques have used omni-directional antennas. The SUs that use an omni-directional antenna cannot determine the sensed PUs exact location. If SUs sense the locations of PUs, they can efficiently utilize the geographic information of the spectrum. Some localization schemes such as the direction of arrival, triangulation or other similar methods used in omnidirectional antennas exchange to message of PU detection among SNs. As a result, it causes harmful interference to the PU. To detect the PUs location more accurately and without harmful interference, a directional antenna can be used for spectrum sensing. Compared with the omni-directional counterpart, the directional technique which needs more radio units has several benefits such as a longer sensing range over the same amount of energy, lower energy consumption with the same sensing range, and fine-grained sensing [6], [18], [24]. In this paper, we propose a directional sensing technique for cognitive radio networks. If we use a directional antenna for spectrum sensing, sensing overhead (sensing time, sensing energy, etc.) can be reduced, and more precise sensing is possible since directional antennas can identify the orientation of the PU. Moreover, the purpose of directional sensing is to identify fine-grained spectrum holes to improve spatial reuse. The rest of this paper is organized as follows. In Section II, relevant spectrum sensing techniques are discussed. Section III describes the basic assumptions for our proposed scheme. Section IV presents the proposed centralized directional spectrum sensing technique. In Section V, we describe the optimization of sensing parameters using the nonlinear optimization technique. The performance of our scheme is evaluated and analyzed in Section VI. Finally, we draw conclusions and suggest future directions in Section VII.

II. Related Work

Spectrum sensing in practice is often compromised by multipath fading, shadowing, and receiver uncertainty issues [4]. To mitigate the impact of these issues, cooperative spectrum sensing has been shown to be an effective method to improve detection performance by exploiting spatial diversity. The main idea of cooperative sensing is to enhance sensing performance by exploiting the spatial diversity in the observations of spatially located CR users [4]. Through cooperation, CR users can share sensing information in order to make a combined decision, which is more accurate compared to individual decisions [12].

To facilitate the analysis of cooperative sensing, we classify cooperative spectrum sensing into two approaches based on how cooperating CR users share the sensing data in the network: *centralized* [5], [11], [13], [34], [36], [40], [44] and *distributed* [8], [10], [14], [19], [27], [32], [37], [42], [45].

In centralized cooperative sensing, a coordinator node called a fusion center (FC) collects the local sensing information from secondary nodes (SNs). After collecting this information, the FC calculates optimized sensing parameters, such as the optimum number of SUs for local sensing, sensing delay, or decision threshold. In [13], the authors proposed a reinforcement learning-based cooperative sensing (RLCS) method to reduce detection overheads and improve detection

This research was supported by the Chung-Ang University Excellent Student Scholarship and Basic Science Research Program through the NRF grant funded by Ministry of Education, Science and Technology (NRF-2010-0024669).

W. Na, J. Yoon, and S. Cho are with the School of Computer Science and Engineering, Chung-Ang University, 156-756 Seoul, South Korea; (E-mail: wsna@uclab.re.kr; jhyoon@uclab.re.kr; srcho@cau.ac.kr).

G. David and G. Nada are with the National Institute of Standards and Technology (NIST); (E-mail: david.griffith@nist.gov; nada.golmie@nist.gov).

[1]The receiver uncertainty problem occurs if an SU is located outside of the primary transmitter (PT) range so that the SU cannot detect the PU's signal. Once the PT transmits to the primary receiver (PR), the transmission of the SU interferes with the reception at the PR.

performance under correlated shadowing. In their scheme, the secondary node acting as the FC interacts with its cooperating neighbors and observes the PU's activity. Furthermore, the FC determines sensing results from its neighbors and learns the behaviors of secondary nodes and PUs. Based on learning information, the FC finds the optimal set of cooperating neighbors with the minimum control traffic and minimizes the overall sensing delay. In [34], the authors proposed a centralized cooperative spectrum sensing technique based on sensing delay and spectrum utilization. They proposed a new metric that describes the sensing performance in terms of sensing delay and spectrum utilization. Based on local sensing results, an FC calculates the optimal number of secondary nodes and local sensing time that can maximize the metric. In [40], the authors considered the optimal combined rule in a centralized cooperative sensing scheme. For a given false alarm probability, they determined the optimal decision threshold that can maximize the expected transmission time while minimizing the interference with PUs.

Unlike the centralized cooperative sensing approaches, distributed cooperative sensing does not rely on an FC for the cooperative decision. In distributed cooperative sensing, each secondary node individually performs local sensing and shares sensing results with other secondary nodes. Based on the shared information, they determine the presence or absence of PUs and efficient sensing parameters. This distributed scheme may require several iterations to reach a unanimous cooperative decision. In [19], the authors proposed a distributed sensing algorithm based on evolutionary/coalition games. In their scheme, each secondary node decides whether to participate in sepctrum sensing or do nothing to save its own energy. Each secondary node selects its action based on its utility history and chooses the strategy that yield the highest utility. Further, secondary nodes sense the channel that carries the most amount of information in order to reduce the uncertainty of the channel status. In [9], the authors proposed an adaptive sensing period optimization scheme for cognitive radio networks based on a genetic algorithm. They aimed to maximize spectrum opportunities as well as minimize the sensing overhead for secondary nodes. In their scheme, the genetic algorithm was used to update the sensing period during each sensing operation. In [14], the authors proposed a cooperative sensing technique based on a greedy heuristic algorithm. In order to reduce the energy consumption for sensing, they attempted to optimize the sensing schedule. In their scheme, each secondary node broadcasts its sensing schedule. If another secondary node receives this information, it determines an optimal sensing schedule by using a greedy heuristic algorithm to reduce the time complexity.

The aforementioned mechanisms attempt to find optimal sensing parameters in a centralized or distributed manner. However, they cannot account for the PU's direction since all secondary nodes perform spectrum sensing with an omni-directional antenna. If each secondary node performs spectrum sensing using a directional antenna, it can increase the accuracy of the PU location (*fine-grained sensing*) with a reduced amount of energy for sensing. By exploiting cooperative sensing, the location information of PUs can be shared among secondary nodes to significantly reduce sensing overhead. There have been a number of studies on directional cognitive radio networks [20], [21], [23], [25], [30], [33], [43] that focus on communication among secondary nodes [20], [30], [33]; the reduction of PU localization error [23], [43] or the design of the directional antenna for cognitive radio networks [21], [25]. However, these types of studies are not applicable to our scenario since we are targeting a spectrum sensing technique with optimized sensing parameters.

Owing to the merits of directional sensing, in the present study, we exploit a directional antenna to sense the spectrum for secondary nodes. Using a directional antenna, we maximize the detection probability while reducing energy consumption for spectrum sensing. Moreover, our scheme can determine optimal sensing parameters, including the sensing period, sensing power, and sensing beams.

III. Basic Assumptions

A. Antenna Model

PUs are assumed to be equipped with an omni directional array based on multiple quasi-omni directional antennas and they communicate omni-directionally [22][2]. We assume that each secondary node including the FC is equipped with a directional antenna, and the antenna is based on a switched beam system with M beam patterns. The secondary node has a single transceiver for the associated directional antenna sector. Furthermore, the PU signal can be detected on the side lobes and thus secondary nodes may cause inaccuracy in determining the direction of the PU. To take this into consideration, we introduce the probability of miss detection and false alarm. Sectors can be used to realize an omni-directional reception function by receiving information from all sectors simultaneously or they can be individually switched for a specific direction. An antenna controller is assumed and to keep track of the direction from which the maximum signal power is received. It then informs the higher layers about the sector of the received signal. Switching within the antenna controller can be achieved by using very fast analog CMOS multiplexers/demultiplexers, which have a transition time less than 217 ns and less than the signal propagation delay [2]. Therefore, the short inter-frame space (SIFS) defined in the 802.11 standard is long enough for an antenna to be switched between transmitting and receiving modes.

B. Primary User Detection

For primary user detection, several schemes, including matched filter, feature detection, and energy detection, generally have been used [3]. In our scheme, we assume that secondary users exploit an energy detection scheme to minimize hardware cost. However, this does not imply that our scheme excludes the use of any other detection scheme for the PU. In energy detection, the ith secondary node SN_i senses the presence/absence of PUs based on the energy of the received signal. The received signal is squared and integrated over the observation interval. Finally, the output of the integrator divided by noise power (SNR) is compared with a certain threshold (or *PU detection sensitivity*) to decide if a PU is present. In other words, if the SNR is higher than the PU detection sensitivity, SN_i decides that a primary user is present [3]. Without loss of generality, an energy detection scheme can generate a miss detection since it is susceptible to uncertainty in noise power. In our scheme, we introduce a PU detection margin R_i, which is defined by the SNR at which a secondary node should alert the primary signal. Therefore, R_i is set to be less than the PU detection sensitivity to accommodate the miss detection probability. For the above reason, we use R_i instead of the PU detection sensitivity in our scheme. Moreover, in the directional sensing scheme, the secondary user can detect the PU signal from more than 2 directions. In this case, the secondary user determines the direction that receives the largest SNR level.

C. Data and Control Channels

In the proposed scheme, we assume that the spectrum of interest is divided into K data channels that are licensed to PUs. To communicate using a data channel, we assume SN_i performs channel sensing during its sensing time for one of K channels to identify any spectrum hole. Let C_i ($C_i \in \{0, 1, \cdots, K-1\}$) represent the channel index to be sensed for SN_i.

In the proposed scheme, we also assume an underlay control channel that uses the entire frequency band (i.e., K channels). The implementation of the underlay control channel for cognitive radio networks has been validated by [38] [3].

With the underlay control channel, secondary nodes can report their sensing results to the FC. The sensing results

[2]We assumed that the proposed technique operates in the mmWave band.

[3]In [38], the underlay control channel is implemented assuming an omni-directional antenna. In our scheme, this is valid since it is possible to operate in the omnidirectional mode by using all the beams of the switched beam antenna.

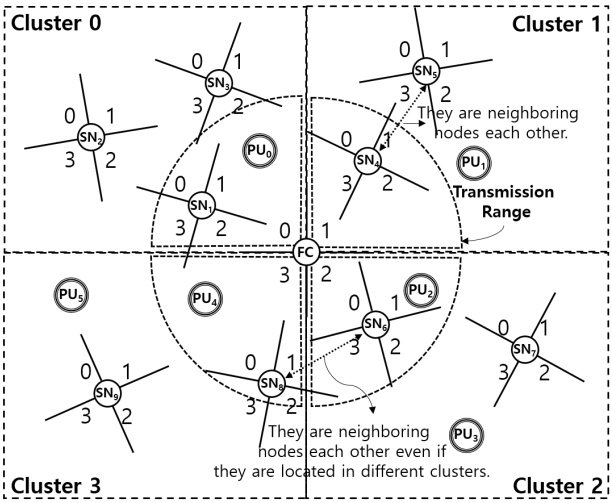

Fig. 1. Example for clustering based on the number of beams of the FC (SN_1–SN_3, SN_4–SN_5, SN_6–SN_7, and SN_8–SN_9 are deployed in clusters 0, 1, 2, and 3, respectively).

include the presence (or absence) of a PU in the channel (C_i) and the direction of the sensed PU. Additionally, the FC can disseminate a command, including optimized sensing parameters, through the underlay channel. However, to remain invisible to the PUs, the transmit power of the underlay channel should be at a level comparable to the noise.

D. Cluster-based Sensing

In the proposed scheme, FC forms multiple clusters, where each cluster corresponds to an FC beam *direction*, as shown in Fig. 1. The rationale behind the cluster being formed by the FC's beam direction is that some secondary nodes are not located in the FC transmission range, such as SN_2, SN_3, SN_5, SN_7, and SN_9 in Fig. 1, and can have connections from the FC through multi-hop links. Sensing tasks can be assigned to each cluster to achieve diversity.

The spectrum sensing function may necessitate quiet periods in the neighborhood of the secondary nodes. If a secondary node SN_i transmits while another secondary node SN_j performs spectrum sensing over the same channel, SN_j decides that at least one PU is present in the channel. This causes a *false alarm* in SN_j. To provide an appropriate quiet period, we assume that all secondary nodes in the same cluster sense the same channel (e.g., C_i) at the same time for the same amount of time (sensing time denoted by t_s).[4] For this reason, nodes are synchronized by the FC.

FC maintains an *SNR table* and a *connectivity matrix* for each cluster. The SNR table stores the detected SNR values of PUs for each channel and node. Therefore, the SNR table forms a three-dimensional matrix in terms of SN_i's, beam indices, and channel indices. The connectivity matrix shows how all secondary nodes are connected to each other in a cluster. To establish the connectivity matrix, each secondary node maintains a local connectivity matrix, which obtains the beam indices at which neighboring nodes are located (referred to as *connectivity information*) by overhearing data frames during the transmission phase. Then, they are transmitted to the FC, which can create the connectivity matrix.

If a secondary node is located far from the FC, we assume that the connectivity information and SNR values of the node are conveyed over multi-hop links. The FC then determines the global spectrum status.

Secondary nodes update their connectivity information when their neighbor nodes transmit connectivity information as well as the SNR value. The FC also updates the SNR table and connectivity matrix when it receives connectivity information.

[4] t_s is the minimum sensing time to detect any PU using the energy detection scheme.

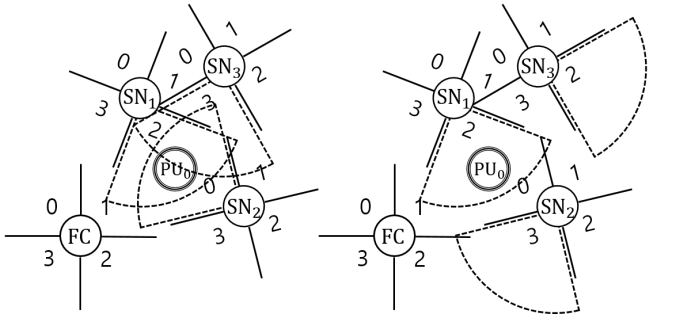

(a) SN_1, SN_2, and SN_3 sense the same area.

(b) SN_2 and SN_3 sense different areas while SN_1 detects PU_0.

Fig. 2. Benefits of a directional cooperative sensing scheme.

IV. Cooperative Directional Sensing

A. Benefits of Cooperative Directional Sensing

As mentioned above, most previous spectrum sensing techniques cannot find the orientation (or direction) of the sensed PU since they use an omni-directional antenna. However, the directional sensing technique determines the beam index at which the sensed PU is located, and thus fine-grained sensing is possible. Moreover, the directional technique has a longer sensing range for the same amount of energy and lower energy consumption for the same sensing range [2].

To facilitate the understanding of how directional cooperative sensing has benefits over its non-cooperative counterpart, we show an example in Fig. 2. Since secondary nodes do not coordinate (or share) sensing tasks in non-cooperative directional sensing, some areas may be unnecessarily sensed by multiple secondary nodes at the same time (energy wastage). For instance, SN_1, SN_2, and SN_3 in Fig. 2 (a) sense the same area in non-cooperative directional sensing. However, secondary nodes in cooperative directional sensing can avoid the above problem since secondary nodes coordinate sensing tasks. In the cooperative counterpart, the FC allocates the sensing tasks of SN_is in such a manner that they sense non-overlapping areas to cover a wider sensing range, thereby reducing the energy consumption, as shown in Fig. 2 (b). Therefore, cooperative sensing can reduce energy consumption and produce faster sensing results compared with non-cooperative sensing.

In summary, the cooperative directional sensing technique has the followings benefits: (1) it enables fine-grained sensing for PUs to realize high location accuracy, (2) it realizes more efficient (in terms of energy and latency) cooperative spectrum sensing among secondary nodes, and (3) it has a longer sensing range for the same energy budget.

B. Proposed Direction Sensing Scheme

In this section, we introduce our proposed cooperative directional sensing technique. In the proposed scheme, each secondary node SN_i except the FC senses a specific spectrum (sensing channel C_i) using its sensing beam B_i and power (sensing range R_i) in its sensing period T_i [5]. These sensing parameters (C_i, B_i, R_i, and T_i) for secondary nodes are assigned by the FC using the optimization scheme described in Section V.

Algorithm 1 shows the pseudo code of a non-FC node for our proposed cooperative sensing scheme. Let T_i, R_i, C_i, and B_i denote the length of the sensing period, PU detection margin, and set of sensing beams for SN_i, respectively. Furthermore, L_r and t_s denote the length of the report phase and sensing time, respectively. We assume that a secondary

[5] In T_i, SN_i performs only one sensing action.

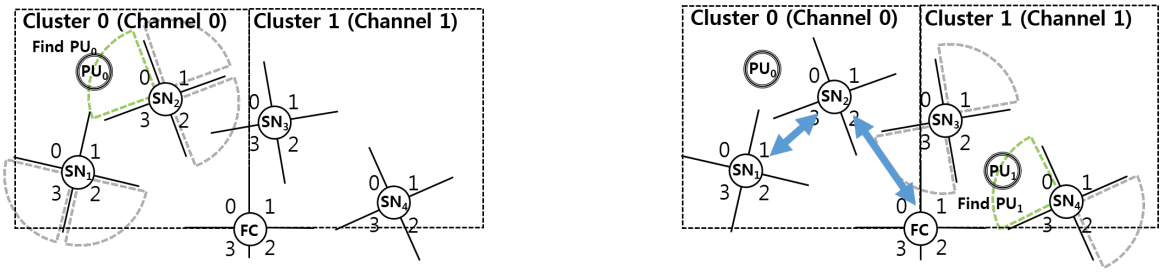

(a) Cluster 0 is in the sensing phase, and cluster 1 is in the transmission phase.

(b) Cluster 0 is in the report phase, and cluster 1 is in the sensing phase.

(c) Cluster 0 is in the transmission phase, and cluster 1 is in the report phase.

(d) Cluster 0 is in the next sensing phase, and cluster 1 is in the transmission phase.

Fig. 3. Example of the proposed directional cooperative sensing.

node has three types of phases: *sensing phase*, *report phase*, and *transmission phase*[6] [7]. In each phase, the secondary node performs the corresponding actions for each phase with time t.

When $0 \leq t \leq t_s$, SN_i is in the sensing phase (*line 12*). In the sensing phase, the secondary node performs spectrum sensing during sensing time t_s. SN_i observes channel C_i with PU detection margin R_i and a set of sensing beams B_i (*line 13*). $\gamma_i^j(C_i)$ is the SNR of PU(s) measured at the jth beam of SN_i with channel C_i. If the signal power received by SN_i is greater than R_i, SN_i determines that at least one PU is present (*line 14*). Then, SN_i finds the beam index (direction of the PU) at which the PU is located (*line 15*).

When $t_s \leq t \leq t_s + L_r$ (*line 17*), SN_i is in the report phase. SN_i transmits a report frame to the FC containing sensing results and receives a command frame from the FC (*lines 18–19*) in the report phase. If SN_i is not located in a 1-hop range from the FC, the SN_i uses a routing algorithm to communicate with the FC. The routing algorithm is beyond the scope of this paper, but relevant material has been studied in [31] and [29] as well as our own previous paper [28]. After receiving a command frame, SN_i blocks the beams with the PU and the beams are indicated in the received command frame during the transmission phase (*line 20*).

After the sensing phase and report phase, SN_i is in the transmission phase until T_i (*line 21*). SN_i transmits or receives data frames to/from other nodes using unblocked beams (*line 22*).[8] At the end of the transmission phase (*line 23*), SN_i updates T_i, R_i, B_i, and C_i from the command frame received during the report phase (*line 24*). Note that C_i remains unchanged for κ sensing periods to reflect the time-varying channel environment. This is addressed in detail in subsection V-D. SN_i unblocks whole blocked beams and resets its timer t to 0 (*lines 25 – 26*).

The FC collects report frames from SN_is and calculates the optimized sensing parameters using the nonlinear optimization technique to maximize the PU detection probability. It also selects beams to be blocked from sensing results based on the connectivity matrix. Information on beams to be blocked are contained in the command frame. The FC disseminates the command frames to all SN_is over the control channel.

Algorithm 1 Cooperative Directional Sensing (Non-FC Nodes)

1: T_i : Length of the sensing period for SN_i;
2: R_i : PU detection margin for SN_i;
3: C_i : Sensing channel for SN_i;
4: B_i : Set of sensing beams for SN_i;
5: L_r : Length of report phase;
6: t_s : Spectrum sensing time;
7: t : Timer;
8: $\gamma_i^j(C_i)$: The SNR of PU(s) measured at the jth beam of SN_i with C_i;
9: $t := 0$;
10: **loop**
11: **if** $0 \leq t \leq t_s$ **then** {// Sensing phase}
12: SN_i senses C_i using R_i and B_i;
13: **if** $\exists \gamma_i^j(C_i) \geq R_i$ **then** {// SN_i detects at least one PU}
14: Find the beam index at which the PU(s) is located
15: **end if**
16: **else if** $t_s \leq t \leq t_s + L_r$ **then** {// Report phase}
17: Transmit report frame to the FC over the control channel;
18: Receive command frame from the FC over the control channel;
19: Block the beams that the PU(s) is located and the beams indicated in the command frame
20: **else if** $t_s + L_r \leq t < T_i$ **then** {// Transmission phase}
21: Transmit or Receive data frames;
22: **else if** $t = T_i$ **then** {// The end of the transmission phase}
23: Update T_i, R_i, B_i, and C_i from command frame;
24: Unblock whole blocked beams;
25: $t := 0$;
26: **end if**
27: **end loop**

[6]Note that a secondary node in the report/transmission phase should vacate the channel within a predefined time similarly in [1] when a PU appears on the channel.

[7]In the transmission phase, the secondary nodes perform fast sensing before transmitting data (or periodically). Fast sensing checks if there is a PU signal within a short time and stops the transmission if a PU signal is detected during that time.

[8]Since the SNs located on boundaries of their cluster interfere with other clusters, we assume that SN_i avoids transmitting over the channels used in adjacent clusters. The channel used in adjacent clusters can be easily calculated. More detailed information is described in subsection V-D

Fig. 3 shows an example of the proposed directional sensing scheme. In this figure, we assume that there are 5 secondary nodes (FC, SN_1-SN_4) and 2 primary users (PU_0 and PU_1) in a given network topology. SN_1 and SN_2 belong to cluster 0, and SN_3 and SN_4 belong to cluster 1.

In Fig. 3(a), cluster 0 starts a new sensing period and is in the sensing phase with sensing parameters allocated in the previous sensing period from the FC. PU_0 is present over channel 0 before the sensing period. SN_1 and SN_2 perform spectrum sensing over channel 0, and SN_2 detects PU_0 using beam 0. Note that SN_1 and SN_2 cannot transmit a frame in t_s owing to the quiet period. Cluster 1 is in the transmission phase. SN_3 and SN_4 communicate data frames.

In Fig. 3(b), cluster 0 is in the report phase. SN_1 and SN_2 then transmit a report frame containing their sensing results to the FC and receive a command frame including new sensing parameters and beams to be blocked from the FC. At the end of the report phase, SN_2 blocks beam 0 at which PU_0 is located. PU_1 begins existing in the area of cluster 1 over channel 1 just before the sensing phase. The SN_is in cluster 1 are allocated according to the current sensing parameters from the FC in the previous sensing period. The SN_is from cluster 1 perform sensing over channel 1. SN_4 detects PU_1 in the direction of beam 0.

In Fig. 3(c), cluster 0 is in the transmission phase when SN_1 and SN_2 communicate data frames, except beam 0 of SN_2. At the end of the transmission phase, SN_1 and SN_2 update the sensing parameters for the next sensing periods. The sensing parameters are contained in the command frame received in the report phase (Fig. 3(b)). Cluster 1 is in the report phase. In the report phase, SN_3 and SN_4 transmit report frames to the FC. The FC is aware that PU_1 is in the range of beam 0 of SN_4, and the range of beam 0 overlaps with beam 2 of SN_3 from the connectivity matrix of cluster 1. Therefore, the FC inserts information to block beam 2 into its command frame for SN_3 and disseminates command frames to all SN_is in cluster 1. Then, SN_3 and SN_4 block beams 2 and 0, respectively, as shown in Fig. 3(d).

In Fig. 3(d), cluster 0 starts the next sensing period with the parameters updated in the previous sensing period. SN_2 detects PU_0 using beam 0 again. Cluster 1 is in the transmission period.

C. Discussion of Multi-hop Routing

In this subsction, we discuss the multi-hop routing scheme for the report phase. As mentioned in subsection III-D, the secondary node, which is located outside the range of the FC, uses a multi-hop routing scheme to transmit (or receive) report (or command) frames within the report phase. For this, we assume that we use an emergency routing algorithm that is very sensitive to QoS and has a very low routing latency.

Additionally, if there are no relaying nodes in the same cluster, SN_i cannot report within the report phase. In this case, the SN_is located in adjacent clusters can function as a relaying node. However, they might be in the report phase or transmission phase, i.e., they may not be able to relay the report frame. To resolve this problem, we assume that each secondary node has two MAC units: one is used for the data channel and the another is used for the control channel. Therefore, the node can relay the report frame (or command frame) through the control channel even if the node is in the transmission phase or sensing phase [26].

V. Optimization of Sensing Parameter

In order to maximize the efficiency of our cooperative spectrum sensing, we optimize the sensing period (T_i), PU detection margin (R_i), channel to sense (C_i), and a set of beams to sense (B_i) for each secondary node using an objective function. B_i can be further described by B_i=[b_i^0, b_i^1, b_i^2, …, b_i^{M-1}]^T, where b_i^j is 1 if the jth beam of SN_i is used for sensing; otherwise, b_i^j is 0. Let N denote the number of secondary nodes in the same cluster. Then, $N \times 1$ vectors of the sensing period, PU detection margin, and channel to sense for the secondary nodes are defined by

$$\underline{T} = [T_0, T_1, T_2, \ldots, T_{N-1}]^T, \quad (1)$$

$$\underline{R} = [R_0, R_1, R_2, \ldots, R_{N-1}]^T, \quad (2)$$

$$\underline{C} = [C_0, C_1, C_2, \ldots, C_{N-1}]^T, \quad (3)$$

respectively, and an $N \times M$ matrix of the set of beams to sense is defined by

$$\mathbf{B} = [B_0, B_1, B_2, \ldots B_{N-1}]^T, \quad (4)$$

where $B_i = \left[b_i^0, b_i^1, \ldots, b_i^{M-1}\right]$.

Our goal is to find an optimum quadruple $(\underline{T}^*, \underline{R}^*, \underline{C}^*, \mathbf{B}^*)$ with an optimization problem defined as

$$\min_{\underline{T},\underline{R},\underline{C},\mathbf{B}} \quad \alpha\left(1 - \Psi(\underline{T}, \underline{R}, \underline{C}, \mathbf{B})\right) + \beta\Phi(\underline{T}, \underline{R}, \underline{C}, \mathbf{B}) \quad (5)$$

$$s.t \quad \alpha + \beta = 1,\ \alpha, \beta \in [0, 1], \quad (6)$$

$$\text{if } C_i = C_j, \text{ then } T_i = T_j, \quad (7)$$

$$T_i > t_s + L_r, \quad (8)$$

$$R_i > 0, \quad (9)$$

$$\forall b_i^j \in \{0, 1\}, \quad (10)$$

where $\Psi(\underline{T}, \underline{R}, \underline{C}, \mathbf{B})$ and $\Phi(\underline{T}, \underline{R}, \underline{C}, \mathbf{B})$ denote the PU detection probability and the sensing overhead in terms of $\underline{T}, \underline{R}, \underline{C}$, and $\mathbf{B}$, respectively. $\Phi(\underline{T}, \underline{R}, \underline{C}, \mathbf{B})$ and $\Psi(\underline{T}, \underline{R}, \underline{C}, \mathbf{B})$ are explained in Sections V-A and V-B, respectively.

A. Analysis of PU Detection Probability

To find the optimum sensing parameters, we calculate the PU detection probability $\Psi(\underline{T}, \underline{R}, \underline{C}, \mathbf{B})$. Let $\Psi_i(T_i, R_i, C_i, B_i)$ denote the probability that SN_i can find at least one PU with T_i, R_i, C_i, and B_i. We assume that SN_i and SN_j independently sense the white space, where $i \neq j, \forall i, j$. Then, $\Psi(\underline{T}, \underline{R}, \underline{C}, \mathbf{B})$ can be calculated as follows:

$$\begin{aligned}\Psi(\underline{T}, \underline{R}, \underline{C}, \mathbf{B}) &= P(\text{ At least one } SN_i \text{ detect any PU}) \\ &= 1 - P(N \text{ nodes cannot find any PU}) \\ &= 1 - \prod_{i=0}^{N-1} \left\{1 - \Psi_i(T_i, R_i, C_i, B_i)\right\}. \end{aligned} \quad (11)$$

From the viewpoint of a single secondary node, i.e., SN_i, the ON-OFF alternating process of a single PU superimposed by ON-OFF processes of the other PUs can be observed as another single merged ON-OFF process, where the ON state indicates that the SNR of the aggregated PU signal is greater than R_i and the OFF state shows otherwise. Therefore, $\Psi_i(T_i, R_i, C_i, B_i)$ can be formulated using the following two hypotheses related to the merged PU signal. The hypotheses are defined as

$$H_0^i : \text{A PU is absent from the viewpoint of } SN_i \quad (12)$$

$$H_1^i : \text{A PU is present from the viewpoint of } SN_i. \quad (13)$$

Let D denote the total duration in which the PU detection probability is to be computed. Fig. 4 shows the timeline of the sensing task. There are $\left\lfloor \frac{D}{T_i} \right\rfloor$[9] sensing periods during D. We assume that D should be greater than T_i (T_i is greater than t_s) in order to calculate the PU detection probability. Let $\Psi_i(\chi_i)$ denote the probability that SN_i detects PU at least once for time duration D, where χ_i is a set of variables T_i, R_i, C_i, and B_i. Then, $\Psi_i(\chi_i)$ is given by

$$\Psi_i(\chi_i) = P_S(B_i, C_i) \left\{ 1 - \prod_{j=0}^{\left\lfloor \frac{D}{T_i} \right\rfloor - 1} \left(1 - P_D^{i,j}(T_i, R_i)\right) \right\} \quad (14)$$

where $P_S(B_i, C_i)$ and $P_D^{i,j}(T_i, R_i)$ denote the probability that SN_i tries to sense a PU using B_i on the channel C_i and SN_i

[9] $\left\lfloor \frac{D}{T_i} \right\rfloor$ is equal to κ, introduced in Section IV-B.

makes a PU detection during the jth sensing period when it selects T_i and R_i, respectively.

We assume that PUs are deployed uniformly and the SU's beam patterns have the same sensing range and are ideally non-overlapping. Therefore, $P_S(B_i, C_i)$ is calculated as follows:

$$P_S(B_i, C_i) = \frac{\text{The number of beams to sense}}{\text{The number of entire beams}} = \frac{\sum_{j=0}^{M-1} b_i^j}{M}. \quad (15)$$

The probability $P_D^{i,j}(T_i, R_i)$ is given by

$$P_D^{i,j}(T_i, R_i) = \left[\begin{array}{l} P\left(\gamma_{i,j} \geq R_i \middle| H_0^i\right) P_j^{T_i}(H_0^i) \\ \quad + P\left(\gamma_{i,j} \geq R_i \middle| H_1^i\right) P_j^{T_i}(H_1^i) \end{array} \right], \quad (16)$$

where $P_j^{T_i}(H_0^i)$ and $P_j^{T_i}(H_1^i)$ denote the probability of H_0^i and H_1^i during the jth sensing period when SN_i selects the sensing period as T_i, respectively. Furthermore, $\gamma_{i,j}$ denotes the SNR measured by SN_i at the jth sensing period.

Now, we consider the PU detection probability under hypothesis H_0^i. The detection probability under H_0^i is equal to the false alarm probability. Therefore, the detection probability under H_0^i is given by [15]

$$P\left(\text{SN}_i \text{ detects a PU} \middle| H_0^i\right) = P_f^i(R_i) = \frac{\Gamma\left(u, \frac{R_i}{2}\right)}{\Gamma(u)}, \quad (17)$$

where $P_f^i(\cdot)$ denotes the false alarm probability, u is the time-bandwidth product, $\Gamma(\cdot)$ is the gamma function, and $\Gamma(\cdot,\cdot)$ is the incomplete gamma function[10].

The detection of at least one PU under hypothesis H_1^i is interpreted to imply that no miss detection occur. $P(\text{SN}_i \text{ detects a PU} \mid H_1^i)$ is given by [15]

$$P\left(\text{SN}_i \text{ detects a PU} \middle| H_1^i\right) = 1 - P_m^i(R_i, C_i, B_i) = Q_u\left(\sqrt{2\gamma_i^j(C_i)}, \sqrt{R_i}\right), \quad (18)$$

where $P_m^i(\cdot,\cdot,\cdot)$ and $Q_u(\cdot,\cdot)$ are the SN_i's miss detection probability and the generalized Marcum Q function, respectively.

In order to detect a PU, it should appear during the $(j-1)$th sensing period and disappear after the jth sensing phase since we assumed that at least a sensing time t_s is required to detect a PU. We denote the time a PU appears by t_a (PU arrival time) and the time a PU disappears as t_d (PU departure time). The time duration for which a PU exists is denoted as t_{on} (i.e., $t_d = t_{on} + t_a$).

[10]the false alarm probability is calculated over the additive white Gaussian noise (AWGN) channel

Therefore, $P_j^{T_i}(H_1^i)$ is calculated as

$$\begin{aligned} P_j^{T_i}(H_1^i) &= P\left(\begin{array}{c}\text{A PU appears in}(j-1)T_i \text{ to } jT_i \\ \text{and disappears after } jT_i + t_s\end{array}\right) \\ &= P\left(t_a \leq jT_i \cap t_d > jT_i + t_s \mid t_a > (j-1)T_i\right) \\ &= P\left(t_a \leq jT_i \cap t_{on} > jT_i + t_s - t_a \mid t_a > (j-1)T_i\right) \\ &= P\left(t_{on} > jT_i + t_s - t_a \mid (j-1)T_i < t_a \leq jT_i\right) P(t_a \leq jT_i) \\ &= \int_{(j-1)T_i}^{jT_i} \left\{1 - F_{on}\left(jT_i + t_s - x\right)\right\} f_{t_a}(x)\, dx F_{t_a}(jT_i), \end{aligned} \quad (19)$$

where f_{t_a}, F_{t_a}, and F_{on} denote the pdf of t_a, CDF of t_a, and CDF of the ON duration, respectively.

$P_j^{T_i}(H_0^i)$ is the probability that SN_i does not find a PU during the jth sensing period. $P_j^{T_i}(H_0^i)$ is naturally caculated from (19) as follows:

$$P_j^{T_i}(H_0^i) = 1 - P_j^{T_i}(H_1^i). \quad (20)$$

Thus, $P_D^{i,j}(T_i, R_i)$ is calculated as (21) from (17), (18), (19), and (20). As a result, $\Psi_i(T_i, R_i, C_i, B_i)$, which is derived from (15) and (21), can be given by (22).

B. Analysis of the Sensing Overhead

In this subsection, we analyze the sensing overhead $\Phi(\underline{T}, \underline{R}, \underline{C}, \mathbf{B})$. $\Phi(\underline{T}, \underline{R}, \underline{C}, \mathbf{B})$ is defined as

$$\Phi(\underline{T}, \underline{R}, \underline{C}, \mathbf{B}) = \sum_{z \in \{s,r,f,c,u\}} \varpi_z \cdot O_z(\underline{T}, \underline{R}, \underline{C}, \mathbf{B}) \quad (23)$$

where $O_z(\underline{T}, \underline{R}, \underline{C}, \mathbf{B})$ and ϖ_z denote the overhead due to spectrum sensing and weight factor, respectively. $O_r(\underline{T}, \underline{R}, \underline{C}, \mathbf{B})$ denotes the overhead due to transmission of sensing results and reception of sensing parameters. $O_f(\underline{T}, \underline{R}, \underline{C}, \mathbf{B})$ denotes unused opportunity due to false alarms. $O_c(\underline{T}, \underline{R}, \underline{C}, \mathbf{B})$ denotes unused opportunity due to incorrect information provided by the other cooperating secondary nodes in a cluster, and $O_u(\underline{T}, \underline{R}, \underline{C}, \mathbf{B})$ denotes unused opportunity due to beam blocking for PU detection (we hereafter use O_z instead of $O_z(\underline{T}, \underline{R}, \underline{C}, \mathbf{B})$).

When a secondary node performs sensing, SN_i loses transmission opportunities during the quiet period. SN_i has to be quiet without transmission to detect PUs during the sensing phase even though PUs are absent. SN_i also consumes its energy during these phases owing to sensing. Therefore, the sensing phase itself is sensing overhead, O_s, given by

$$O_s = \sum_{i=0}^{N-1} \left\lfloor \frac{D}{T_i} \right\rfloor t_s. \quad (24)$$

SN_i also loses transmission opportunities to transmit sensing results and to receive sensing parameters. Hence, the report phase itself is a report overhead, O_r, given by

$$O_r = \sum_{i=0}^{N-1} \left\lfloor \frac{D}{T_i} \right\rfloor L_r. \quad (25)$$

$$\begin{aligned} P_D^{i,j}(T_i, R_i) = {} & \frac{\Gamma\left(u, \frac{R_i}{2}\right)}{\Gamma(u)} \left[1 - \int_{(j-1)T_i}^{jT_i} \left\{1 - F_{on}\left(jT_i + t_s - x\right)\right\} f_{t_a}(x)\, dx F_{t_a}(jT_i)\right] \\ & + Q_u\left(\sqrt{2\gamma_i^j(C_i)}, \sqrt{R_i}\right) \int_{(j-1)T_i}^{jT_i} \left\{1 - F_{on}\left(jT_i + t_s - x\right)\right\} f_{t_a}(x)\, dx F_{t_a}(jT_i) \end{aligned} \quad (21)$$

$$\Psi_i(T_i, R_i, C_i, B_i) = \frac{\sum_{j=0}^{M-1} b_i^j}{M} \left\{1 - \prod_{j=0}^{\left\lfloor \frac{D}{T_i} \right\rfloor - 1} \left(1 - \left(\begin{array}{l} \frac{\Gamma\left(u, \frac{R_i}{2}\right)}{\Gamma(u)} \left\{1 - \int_{(j-1)T_i}^{jT_i} \left\{1 - F_{on}\left(jT_i + t_s - x\right)\right\} f_{t_a}(x)\, dx F_{t_a}(jT_i)\right\} \\ \quad + Q_u\left(\sqrt{2\gamma_i^j(C_i)}, \sqrt{R_i}\right) \int_{(j-1)T_i}^{jT_i} \left\{1 - F_{on}\left(jT_i + t_s - x\right)\right\} f_{t_a}(x)\, dx F_{t_a}(jT_i) \end{array} \right)\right)\right\} \quad (22)$$

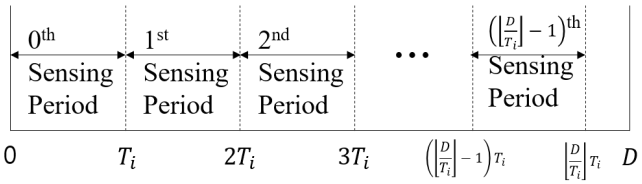

Fig. 4. Timeline of the sensing tasks.

Before defining O_f, O_c and O_u, we consider the following. First, we consider the PU status. The probability that a PU is absent is given as

$$P_{\text{absent}}^{PU} = P(\text{PU is absent}) = \frac{E[OFF]}{E[ON]+E[OFF]} = \frac{\int_0^\infty t f_{off}(t)dt}{\int_0^\infty t f_{on}(t)dt + \int_0^\infty t f_{off}(t)dt} \quad (26)$$

where $f_{off}(\cdot)$ and $f_{on}(\cdot)$ are pdfs of the OFF duration and ON duration, respectively. Similar to (26), the probability that a PU is present is derived as

$$P_{\text{present}}^{PU} = P(\text{PU is present}) = \frac{E[ON]}{E[ON]+E[OFF]} = \frac{\int_0^\infty t f_{on}(t)dt}{\int_0^\infty t f_{on}(t)dt + \int_0^\infty t f_{off}(t)dt}. \quad (27)$$

Next, we consider the fraction of unused time. $\mu(c,t)$ is introduced to denote the average fraction of the OFF duration during t on channel c.

In our scheme, SN_i blocks a beam where at least one PU is detected to avoid interference with the PU. However, this operation is unnecessary if a false alarm occurs, in which case SN_i loses the transmission opportunity due to false alarms. O_f is the unused opportunity (unused time fraction) during the transmission phase resulting from unused beams due to false alarms. Fig. 5(c) depicts an example of O_f. Therefore, O_f can be calculated as

$$O_f = \sum_{i=0}^{N-1}\left[\mu(C_i,\widetilde{T}_i)P_{\text{absent}}^{PU}\sum_{k=0}^{M-1}\frac{b_i^k P_f^i(R_i)}{M}\left\lfloor\frac{D}{T_i}\right\rfloor\right] = \sum_{i=0}^{N-1}\left[\mu(C_i,\widetilde{T}_i)P_{\text{absent}}^{PU}\sum_{k=0}^{M-1}\frac{b_i^k \frac{\Gamma\left(u,\frac{R_i}{2}\right)}{\Gamma(u)}}{M}\left\lfloor\frac{D}{T_i}\right\rfloor\right], \quad (28)$$

where $\widetilde{T}_i$ denotes the length of the transmission phase ($\widetilde{T}_i = T_i - t_s - L_r$). Here, (28) considers only beams in the sensing operation. Beams that are not engaged in sensing will be reflected in O_c.

FC collects sensing results from and sends sensing parameters (including B_is) to SN_is. The SN_is then block all beams, including the beams with false alarms, such that $b_i^k = 0$. O_c is the unused opportunity during the transmission phase resulting from the unused beams due to false alarms from cooperating nodes. Fig. 5(d) describes an example of O_c. Therefore, O_c can be calculated as (29). $|\cdot|$ denotes the absolute value, and N_i^k is the number of cooperating nodes of SN_i on beam k of SN_i.

If SN_i detects at least one PU or receives PU information from the FC, it blocks the corresponding beams. Even though PUs disappear during the transmission phase, SN_i still blocks the beam until the end of the sensing period. O_u denotes the unused time fraction during the transmission phase after PUs are detected. An example of this unused opportunity is described in Fig. 5(e). Therefore, O_u can be calculated as (30).

From (23), (24), (25), (28), (29), and (30), $\Phi(\underline{T},\underline{R},\underline{C},\mathbf{B})$ is calculated as (31) where $\varpi_z = 1/(5\cdot\max(O_z))$. Since (31) is the summation of sensing overhead of each SN_i, (31) is decomposed as

$$\Phi(\underline{T},\underline{R},\underline{C},\mathbf{B}) = \frac{1}{N}\cdot\sum_{i=0}^{N-1}\Phi_i(\underline{T},\underline{R},\underline{C},\mathbf{B}), \quad (32)$$

where $\Phi_i(\underline{T},\underline{R},\underline{C},\mathbf{B})$ denotes the sensing overhead of SN_i.

C. Optimization of $\underline{T}$ and $\underline{R}$

In this subsection, we determine $\underline{T}^*$ and $\underline{R}^*$ from the optimization problem in (5) using a nonlinear optimization technique. We will solve this problem by the *trust region method* [41]. However, to obtain insight into how our optimization process is achieved, we introduce some reasonable approximations and assumptions [8], [13], [17], [34].

1) Problem Reduction: First, for a smooth approximation, to the term $\left\lfloor\frac{D}{T_i}\right\rfloor$ is approximated as

$$\left\lfloor\frac{D}{T_i}\right\rfloor \approx \frac{D}{T_i}. \quad (33)$$

The gap of values between the orginal one and the approximated one is below 0.1% in the objective function. Hereafter, we denote the approximated $\left\lfloor\frac{D}{T_i}\right\rfloor$ by $\widetilde{\frac{D}{T_i}}$.

We assume t_{on} and t_a follow an exponential distribution with rate parameters λ_{on} and λ_a, respectively [8], [13], [17], [34]. From the memoryless property of the exponential distribution, (19) is rewritten as

$$P_j(H_1^i) = P(t_a \le jT_i \cap t_d > jT_i + t_s | t_a > (j-1)T_i) = P(t_a \le T_i \cap t_d > T_i + t_s). \quad (34)$$

From (34), we observe that $P_j(H_1^i)$ is independent of j. Then, $P_j(H_1^i) = P_{j'}(H_1^i),\ \forall j \ne j'$. This implies that the $P_j(H_0^i)$s are also the same for every j. $P_j(H_1^i)$ and $P_j(H_0^i)$ are assumed to be constant. $P_f^i(R_i)$ and $P_m^i(R_i,C_i,B_i)$ are assumed to be fixed, as in subsection V-A. Therefore,

$$P_D^{i,j} = P_D^{i,j'},\ \forall j = j'. \quad (35)$$

From the assumption, (11) is rewritten as

$$\Psi_i(\chi_i) = \frac{\sum_{j=0}^{M-1}(b_i^j)}{M}\left\{1-\left(1-P_D^{i,j}\right)^{\widetilde{\frac{D}{T_i}}}\right\}. \quad (36)$$

(18) is too complicated to calculate for the modified Bessel function in the Marcum Q function. Thus, the modified Bessel function is approximated as

$$I_\alpha(x) \approx \frac{e^x}{\sqrt{2\pi x}}, \quad (37)$$

for $x \gg \alpha$. In the case of $\alpha = 1$, the error between the original function and the approximation is below 5% when $x > 15$. The errors from (33) and (37) are sufficiently small and negligible.

In subsection V-B, we introduced $\mu(c,t)$ to denote the average fraction of the OFF duration. The OFF duration on channel c is assumed to be distributed exponentially with a rate parameter $\lambda_{off|c}$. Then, $\mu(c,t)$ is given as [17, (3)]

$$\mu(c,t) = \frac{1}{\lambda_{off|c}}\left\{1-\frac{1-e^{-\lambda_{off|c}t}}{\lambda_{off|c}t}\right\}. \quad (38)$$

The dimensionality for the domain of the $\underline{T}$ and $\underline{R}$ optimization problem is $2N$ (N T_is and N R_is). A constraint (7) is interpreted as implying that all T_i have to be the same when in the same cluster (due to the quiet period). Under fixed $\underline{C}^*$ and $\mathbf{B}^*$, $\underline{T}$ can be substituted by a scalar variable τ. Then, the objective function (5) is rewritten with respect to τ and $\underline{R}$ as

$$f(\tau,\underline{R}) = \alpha\{1-\Psi(\tau,\underline{R},\underline{C}^*,\mathbf{B}^*)\} + \beta\Phi(\tau,\underline{R},\underline{C}^*,\mathbf{B}^*) = \alpha\overline{\Psi}^*(\tau,\underline{R}) + \beta\Phi^*(\tau,\underline{R}), \quad (39)$$

where $\overline{\Psi}^*(\cdot)$ denotes $1-\Psi(\cdot)$. The new dimensionality of the problem is $N+1$ (almost half of the original one).

In our objective function, we observe that $\Phi^*(\tau,\underline{R})$ (hereafter $\overline{\Phi}^*$) dominates in finding an optimal point since the range

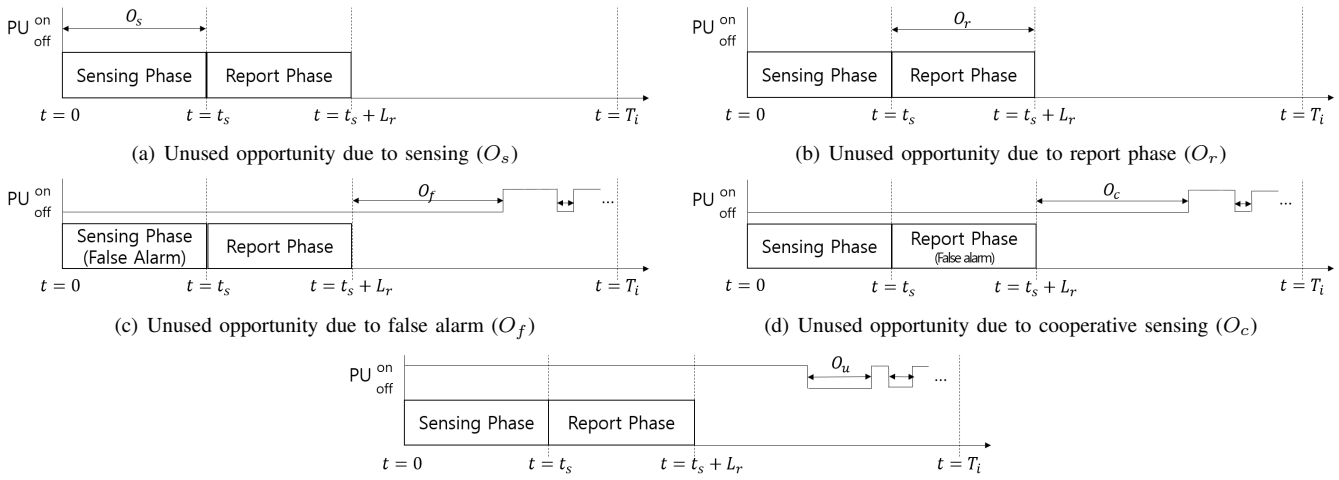

(a) Unused opportunity due to sensing (O_s)

(b) Unused opportunity due to report phase (O_r)

(c) Unused opportunity due to false alarm (O_f)

(d) Unused opportunity due to cooperative sensing (O_c)

(e) Unused opportunity due to PU detection (O_u)

Fig. 5. Examples for timelines of each O_z.

of $\overline{\Psi}^*$ is smaller than the range of $\overline{\Phi}^*$[11]. To solve the above problem, α and β from (39) should have values that balance between the ranges of $\overline{\Psi}^*$ and Φ^*. We use two variables

$$\Delta\overline{\Psi}^* = \max \overline{\Psi}^* - \min \overline{\Psi}^*, \tag{40}$$

$$\Delta\Phi^* = \max \Phi^* - \min \Phi^*. \tag{41}$$

It is clear that the ranges of $\frac{1}{\Delta\overline{\Psi}^*}\overline{\Psi}^*$ and $\frac{1}{\Delta\Phi}\Phi^*$ are identical. Therefore, we propose α and β as

$$\alpha = \frac{\Delta\Phi^*}{\Delta\overline{\Psi}^* + \Delta\Phi^*}, \tag{42}$$

$$\beta = \frac{\Delta\overline{\Psi}^*}{\Delta\overline{\Psi}^* + \Delta\Phi^*} \tag{43}$$

where (42) and (43) satisfy (6).

From the above approximations and assumptions, we can show our problem has a global optimal point $\underline{X}$, which is an $N+1$-component vector, defined as

$$\underline{X} = [\tau, R_0, R_1, \cdots, R_{N-1}]^T, \tag{44}$$

where $\underline{X}$ replaces τ and $\underline{R}$.

τ includes the length of the sensing phase, the report phase, and the transmission phase (T_i). The transmission phase is essential since a CRN needs to communicate. However, there is no length for the transmission phase in (8). SN_i uses an energy detector for spectrum sensing. A spectrum sensing result (energy) is always larger than 0 for noise. Therefore, the ranges of τ and R_is are redefined as

$$\tau \in [t_s + L_r + \epsilon_T, T_{\max}], \tag{45}$$

$$R_i \in [\epsilon_R, R_{\max}], \tag{46}$$

where ϵ_T and ϵ_R are sufficiently small positive constants.

Theorem 1. *The objective function f(X) is a convex function.*

Proof. See Appendix **??**. ■

Karush-Khun-Tucker (KKT) conditions can be used to find the optimality of our optimization problem. Note that KKT conditions are necessary conditions of optimality for nonlinear optimization [46]. The Lagrange function for the objective function thus becomes

$$\begin{aligned} &L(\underline{X}, \Xi) = \\ &f(\underline{X}) + \xi_1(-\tau + t_s + L_r + \epsilon_T) + \xi_2(\tau - T_{max}) \\ &+ \sum_{i=0}^{N-1} \left[\xi_{2i+3}(-R_i + \epsilon_R) + \xi_{2i+4}(R_i - R_{\max})\right], \end{aligned} \tag{47}$$

where $\xi_i (i = 1, 2, \ldots, 2N+2)$ denotes a Lagrange multiplier.

The KKT conditions of our objective problem are given by [46]

$$t_s + L_r + \epsilon_T \leq \tau^* \leq T_{\max}, \tag{48}$$

$$\epsilon_R \leq R_i^* \leq R_{\max}, \forall R_i \tag{49}$$

$$\xi_d \geq 0, \forall \xi_d \tag{50}$$

$$\xi_1(-\tau^* + t_s + L_r + \epsilon_T) = 0, \tag{51}$$

$$\xi_2(\tau^* - T_{max}) = 0, \tag{52}$$

$$\xi_{2i+3}(-R_i^* + \epsilon_R) = 0, \forall i, \tag{53}$$

$$\xi_{2i+4}(R_i^* - R_{\max}) = 0, \forall i, \tag{54}$$

$$\bigtriangledown_{\underline{X}} L(\underline{X}^*, \Xi) = 0, \tag{55}$$

where $\bigtriangledown_{\underline{X}}$ is the derivative with respect to $\underline{X}$, $\underline{X}^*$ is the optimal $\underline{X}$ and $\Xi = [\xi_1, \xi_2, \cdots, \xi_{2N+2}]^T$.

From (47), the Lagrange form of our objective function is a constrained problem. Therefore, the optimization problem

[11]The ranges of both $\overline{\Phi}^*$ and $\overline{\Psi}^*$ are 0 to 1. However, $\overline{\Psi}^*$ is very small because it denotes the probability that all SUs will not find any PUs.

$$\begin{aligned} O_c &= \sum_{i=0}^{N-1} \left[\mu(C_i, \widetilde{T}_i) P_{\text{absent}}^{PU} \sum_{k=0}^{M-1} \frac{\left|1 - b_i^k\right| \left\{1 - \left(1 - P_f^i(R_i)\right)^{N_i^k}\right\}}{M} \left\lfloor \frac{D}{T_i} \right\rfloor \right] \\ &= \sum_{i=0}^{N-1} \left[\mu(C_i, \widetilde{T}_i) P_{\text{absent}}^{PU} \sum_{k=0}^{M-1} \frac{\left|1 - b_i^k\right| \left\{1 - \left(1 - \frac{\Gamma\left(u, \frac{R_i}{2}\right)}{\Gamma(u)}\right)^{N_i^k}\right\}}{M} \left\lfloor \frac{D}{T_i} \right\rfloor \right], \end{aligned} \tag{29}$$

$$O_u = \sum_{i=0}^{N-1}\left[\mu(C_i,\widetilde{T}_i)P_{\text{present}}^{PU}\sum_{k=0}^{M-1}\left[\frac{b_i^k\{1-P_m^i(R_i,C_i,B_i)\}+\left|1-b_i^k\right|\{1-P_m^i(R_i,C_i,B_i)^{N_i^k}\}}{M}\right]\left\lfloor\frac{D}{T_i}\right\rfloor\right] \tag{30}$$

$$= \sum_{i=0}^{N-1}\left[\mu(C_i,\widetilde{T}_i)P_{\text{present}}^{PU}\sum_{k=0}^{M-1}\left[\frac{b_i^k Q_u\left(\sqrt{2\gamma_i^j(C_i)},\sqrt{R_i}\right)+\left|1-b_i^k\right|\left\{1-\left\{1-Q_u\left(\sqrt{2\gamma_i^j(C_i)},\sqrt{R_i}\right)\right\}^{N_i^k}\right\}}{M}\right]\left\lfloor\frac{D}{T_i}\right\rfloor\right]$$

$$\Phi(\underline{T},\underline{R},\underline{C},\mathbf{B}) = \varpi_s\sum_{i=0}^{N-1}\left\lfloor\frac{D}{T_i}\right\rfloor t_s + \varpi_r\sum_{i=0}^{N-1}\left\lfloor\frac{D}{T_i}\right\rfloor L_r + \varpi_f\sum_{i=0}^{N-1}\left[\mu(C_i,\widetilde{T}_i)P_{\text{absent}}^{PU}\sum_{k=0}^{M-1}\frac{b_i^k\frac{\Gamma\left(u,\frac{R_i}{2}\right)}{\Gamma(u)}}{M}\left\lfloor\frac{D}{T_i}\right\rfloor\right]$$

$$+\varpi_c\sum_{i=0}^{N-1}\left[\mu(C_i,\widetilde{T}_i)P_{\text{absent}}^{PU}\sum_{k=0}^{M-1}\frac{\left|1-b_i^k\right|\left\{1-\left(1-\frac{\Gamma\left(u,\frac{R_i}{2}\right)}{\Gamma(u)}\right)^{N_i^k}\right\}}{M}\left\lfloor\frac{D}{T_i}\right\rfloor\right] \tag{31}$$

$$+\varpi_u\sum_{i=0}^{N-1}\left[\mu(C_i,\widetilde{T}_i)P_{\text{present}}^{PU}\sum_{k=0}^{M-1}\left[\frac{b_i^k Q_u\left(\sqrt{2\gamma_i^j(C_i)},\sqrt{R_i}\right)+\left|1-b_i^k\right|\left\{1-\left\{1-Q_u\left(\sqrt{2\gamma_i^j(C_i)},\sqrt{R_i}\right)\right\}^{N_i^k}\right\}}{M}\right]\left\lfloor\frac{D}{T_i}\right\rfloor\right]$$

needs to be converted from the constrained problem to an unconstrained problem using the logarithmic barrier method [16]. The logarithmic barrier method forms a barrier on the objective function using the constraints in (48) and (49). Then, our problem is converted to the following:

$$\min \widehat{f}(\underline{X}) = \begin{bmatrix} f(\underline{X}) - \log(L_t-\epsilon_T) - \log(-\tau+T_{\max}) \\ -\sum_{i=0}^{N-1}\{\log(R_i-\epsilon_R)+\log(-R_i+R_{\max})\}\end{bmatrix}, \tag{56}$$

where L_t and $\widehat{f}(\cdot)$ denote $\tau - t_s - L_r$ and the converted unconstrained objective function, respectively.

Similar to the previous step, the KKT conditions of (56) are given by

$$\nabla_{\underline{X}}\widehat{f}(\underline{X}^*) = 0. \tag{57}$$

2) Proposed Optimization Algorithm: (57) is too complicated to solve analytically. There is at least one minimum point according to Theorem 1. We introduce a numerical optimization algorithm based on the gradient descent method of which the time complexity of which is small [35].

We define the *numerical gradient* since computing the gradient of the objective function has a large complexity.

Definition 1. *The numerical gradient* $\tilde{\nabla}$ *is defined as*

$$\tilde{\nabla} g(\underline{Y}) = \sum_{\forall k}\frac{g(\underline{Y}+h\mathbf{a}_k)-g(\underline{Y}-h\mathbf{a}_k)}{2h}\mathbf{a}_k, \tag{58}$$

where $g(\cdot)$*,* $\underline{Y}$*, and* h *are a function, a vector, and a step size, respectively.* $\mathbf{a}_k$ *is a column vector, whose size is the same as the size of* $\underline{Y}$*, consisting of 0s except for the* k*th element (the* k*th element is 1).*

We calculate the numerical gradient instead of the gradient because the differentiation of the objective function is highly complex. The algorithm is described in Algorithm 2.

Algorithm 2 Numerical Gradient Method for T and R

$\underline{X}^0$: The starting point (input)
$\underline{X}^*$: The optimal solution (output)
$\underline{X}_k$: The point at the kth iteration
δ: The tolerance
h: The numerical gradient step size
$k := 0$
$\underline{X}_k := \underline{X}^0$;
$\gamma := [\frac{h}{T_{max}-t_s-L_r-\epsilon_T},\ \frac{h}{R_{max}-\epsilon_R},\ ...,\ \frac{h}{R_{max}-\epsilon_R}]^T$ // The size of γ is $(N+1)\times 1$
while $\tilde{\nabla}\hat{f}(\underline{X}_k) > \delta$ **do**
  $\underline{X}_{k+1} := \underline{X}_k - \gamma\cdot\tilde{\nabla}\hat{f}(\underline{X}_k)$;
  $k := k+1$
  if $\underline{X}_k$ exceeds the left edge of (48) and (49) **then**
    $\underline{X}_k := [t_s+L_r+\epsilon_T, \epsilon_R,\ ...,\ \epsilon_R]^T$;
    break;
  else if $\underline{X}_k$ exceeds the right edge of (48) and (49) **then**
    $\underline{X}_k := [T_{max}, R_{max},\ ...,\ R_{max}]^T$;
    break;
  end if
end while
$\underline{X}^* := \underline{X}_k$

D. Selection of $\mathbf{B}^*$ *and* $\underline{C}^*$

In this subsection, we select optimized parameters B_i and C_i. Since B_i and C_i are discrete variables, we cannot use the non-linear optimization technique used for finding $\underline{T}^*$ and ${\underline{R_i}}^*$. Therefore, this paper proposes an algorithm to select B_i and C_i.

All of the secondary nodes, which are located in the same cluster, sense the same channel and have the same κ, as stated in subsection IV-B. The FC selects a new C_i after the κth sensing period from the new C_i selection. The new C_i is selected as $\{(C_i+1) \mod K\}$.

The goal of objective function (5) is to maximize the PU detection probability and minimize the sensing overhead. We can achieve this goal by selecting beams with higher $\gamma_i^j(C_i)$ and minimizing the number of sensing beams from (22) and (31). In this paper, we propose an algorithm to select $\mathbf{B}^*$. Recall that the FC maintains SNR tables, as stated in Section III-D. There are K SNR matrices (for each data channel) of size $N\times M$ (same size as $\mathbf{B}$). The proposed algorithm selects non-overlapped ranges of beams with higher

TABLE I
SIMULATION PARAMETERS.

Parameter	Value
Topology Size	1 km x 1 km
Data Frame Size	1024 Bytes
Traffic Rate of SN_i	0.1 sec
Operating Frequency	60 GHz
Energy Consumption per Sensing	0.4 mJ
Number of Beams M	2-16
Number of PUs	1-10
Number of Secondary Nodes	25
The Length of Report Phase L_r	0.04 sec[12]
The Length of Sensing Phase t_s	0.01 sec
$1/\lambda_{on}$	0.5-5.5
$1/\lambda_{off}$	2.0
$1/\lambda_a$	0.5-4.5

SNR using an SNR matrix.

First, the FC initializes as all b_i^j as 1 and sorts the b_i^js corresponding channel in descending order of $\gamma_i^j(C_i)$. Then, the FC starts to determine each beam to perform sensing from the first b_i^j. The FC checks whether there are beams overlapping with the beam corresponding to the selected b_i^j using the connectivity matrix. If there are overlapped beams (connected beams in the in connectivity matrix), the b_i^js corresponding to the beams are set to 0. This process is skipped if the corresponding $b_i^j = 0$ and repeated until the last b_i^j. By the above algorithm, the FC can select beams with higher SNR and minimize the number of sensing beams by selecting non-overlapping beams.

VI. PERFORMANCE EVALUATION

In this section, we evaluate the performance of our proposed directional cooperative sensing scheme. We developed a simulator using the OPNET modeler. The simulation parameters are listed in Table I. To measure the effectiveness of the proposed scheme, we evaluate the following performance metrics.

- **Aggregate Throughput of Secondary Nodes (Mbps):** Total data traffic of all secondary nodes in bits transferred successfully from all secondary nodes divided by time
- **Energy Consumption for Sensing (mJ):** Total energy consumption from all secondary nodes for sensing
- **Channel Utilization (%):** The percentage of time that a channel is occupied by secondary nodes in the entire time
- **Sensing Overhead:** The summation of the sensing overhead, as defined in (31) divided by time

To evaluate the effectiveness of our proposed scheme, we compared the performance of our proposed scheme, non-optimized schemes (directional sensing), and an omni-directional sensing scheme. The difference between our proposed scheme and the non-optimized scheme is whether the sensing parameters $\underline{T}$, $\underline{R}$, $\underline{C}$, and $\mathbf{B}$ are optimized. Additionally, in the omni-directional sensing scheme, the sensing parameters are optimized based on our optimization technique ($\underline{T}$ and $\underline{R}$)

Moreover, for directional sensing, the PU signal can be detected on the side lobe, and secondary nodes may be mistaken for the position of the PU (due to multipath propagation). Because of the error in estimating the PU location, the false probability of alarm in directional sensing is greater than in omni-directional sensing. To compensate for this probability, we adjusted the false alarm probability to a similar level as in reference [43] for our simulation.

[12]If the length of L_r is short in a dense environment, there is a possibility that optimization may not work properly owing to report message collision. For this purpose, we set 0.04 s as a fairly fixed L_r.

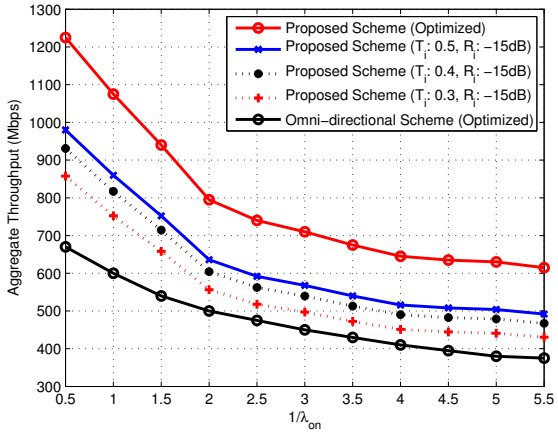

Fig. 6. Aggregate throughput vs. $1/\lambda_{on}$.

A. Simulation Setup

We simulate a system consisting of multiple clusters of 24 SN_is and one FC. The number of clusters is the same with as the number of beams per secondary node. The nodes in these networks are uniformly distributed over 1×1 km^2 . Secondary nodes consume 0.4 mJ per spectrum sensing. We adopt an inter-arrival time of SN_i from an upper-layer as 0.1 s. SN_i is in the report phase for 0.03 s, and we assume that the FC takes 5 μs to find the optimal value.

We introduced the time-bandwidth product u in Section V to calculate some functions. u heavily affects the functions e.g., through R_i-axis scaling, which affects the result of computation. u is defined as $u = Wt_s$. We set the bandwidth per data channel W to 1000 Hz and the length of the sensing phase t_s to 0.01 s. Then, u is calculated as 1, which is a reasonable value for calculating $\underline{R}^*$.

We measure the performance of our proposed scheme in the following three scenarios: (1) $1/\lambda_{on}$ is variable ($1/\lambda_{on} \in [0.5, 5.5]$), (2) $1/\lambda_a$ is variable ($1/\lambda_a \in [0.5, 4.5]$), and (3) the number of SU's beams (M) is variable ($M \in \{2, 4, 6, 8, 10, 12, 14, 16\}$). The simulation parameters are summarized in Table I.

The number of PUs is not fixed in Table I. However, we state that the ON-OFF alternating process of multiple PUs is superimposed on a single ON-OFF alternating process, as in Section V. The number of PUs affects the values of λ_{on} and λ_a. Therefore, we do not consider the number of PUs as a scenario.

We compared each metric for each SN_i. The definitions of $1/\lambda_{on}$ and $1/\lambda_a$ are the average of the ON duration of PUs and the inter-arrival time of PUs, respectively. From the definitions, however, $1/\lambda_{on}$ and $1/\lambda_a$ are interpreted as how long PUs are on and how often PUs are present, respectively.

B. Simulation Results

We first evaluate a metric aggregate throughput. Figs. 6, 7, and 8 show the simulation results of the aggregate throughput versus $1/\lambda_{on}$, $1/\lambda_a$, and the number of beams, respectively. We observe that the aggregate throughput decreases as $1/\lambda_{on}$ increases since the time occupied by PUs is longer. Contrary to the previous case, the aggregate throughput increases as $1/\lambda_a$ increases, as shown in Fig. 7. A larger $1/\lambda_a$ does not indicate a longer occupation by PUs. The FC optimizes $\underline{T}$ longer when $1/\lambda_{on}$ is smaller and $1/\lambda_a$ is larger to maximize PU detection probability and minimize unused opportunity. A larger $\underline{T}$ means a smaller number of sensing periods. Frequent sensing causes lower aggregate throughput due to more quiet periods, sensing overhead, and report overhead. We also observed that the directional sensing technique outperforms the omni-directional sensing tehchnique for all ranges. Although, the

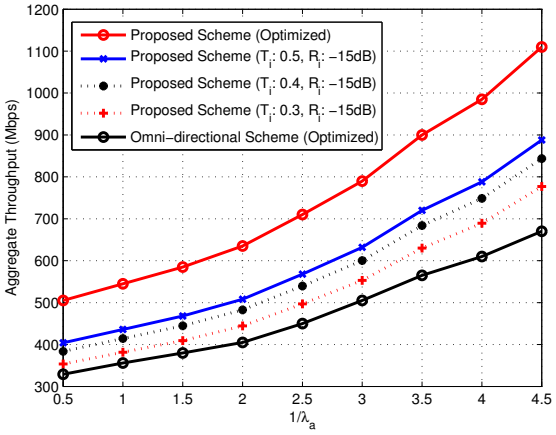

Fig. 7. Aggregate throughput vs. $1/\lambda_a$.

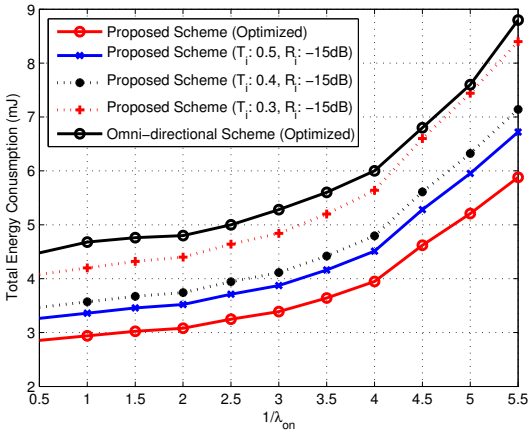

Fig. 9. Energy consumption of SNs vs. $1/\lambda_{on}$.

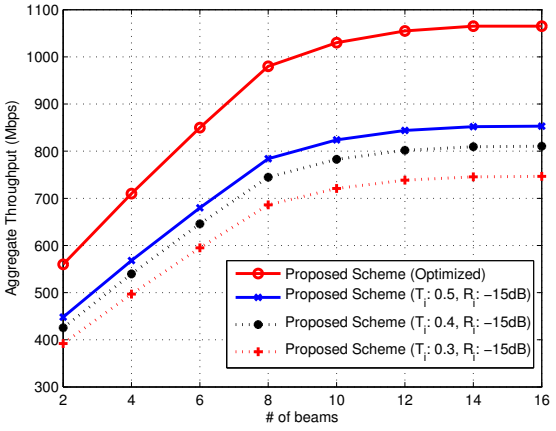

Fig. 8. Aggregate throughput vs. the number of beams.

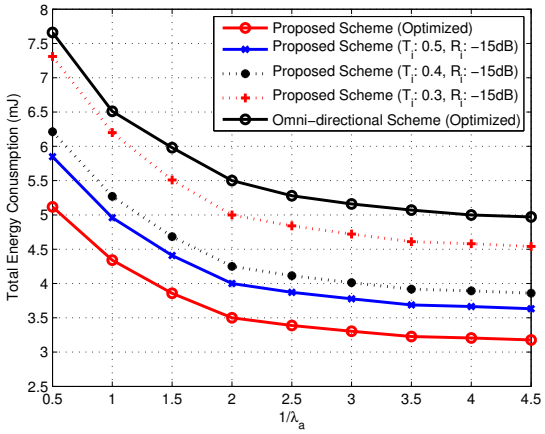

Fig. 10. Energy consumption of SNs vs. $1/\lambda_a$.

directional sensing technique causes false alarm, secondary nodes transmit more data with spatial resources.

"How long" ($1/\lambda_{on}$) and "how often" ($1/\lambda_a$) are independent, i.e., $1/\lambda_a$ does not affect $1/\lambda_{on}$. Therefore, there are no abnormal channel utilization increases following $1/\lambda_a$. The FC actually optimally maximizes channel utilization. Furthermore, the channel utilization increases as the number of beams increases. This is because a narrower beam stimulates spatial reuse, and communication is possible by avoiding the PU signal.

The aggregate throughput increases as the number of beams increases. This is because a narrower beam stimulates spatial reuse in our scheme and allows more fine-grained sensing. As a result, the SNs have more opportunity to transmit simultaneously. One interest finding is that the slope of throughput decreases as the number of beams increases after $M = 10$. Since the PU transmits in all directions, the number of beams that cannot be used increase even if the beam is narrowed. As a result, even if the number of beams increases by 10 or more, the spatial reuse cannot be maximized. The aggregate throughput of the proposed scheme demonstrates the best performance among the compared schemes.

Now, we measure the metric energy consumption. Figs. 9, 10, and 11 show the simulation results of the energy consumption of SN_is versus $1/\lambda_{on}$, $1/\lambda_a$, and the number of beams, respectively. The energy consumption includes only the energy consumed for sensing. We observe that the energy consumption increases as $1/\lambda_{on}$ increases since SN_i performs more frequent spectrum sensing. On the other hand, the energy consumption decreases as $1/\lambda_a$ increases. The above two

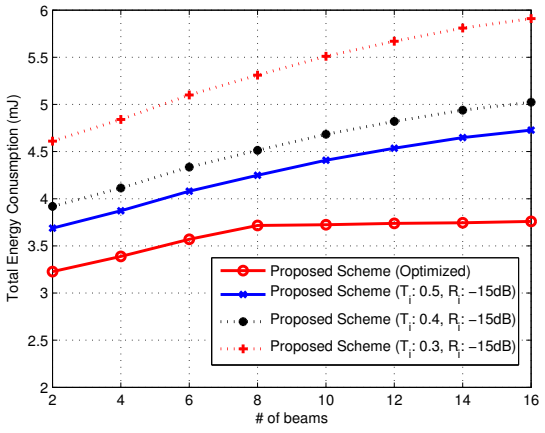

Fig. 11. Energy consumption vs. the number of beams.

cases show opposite results to cases of aggregate throughput where there are less sensing phases with small $1/\lambda_{on}$ and large $1/\lambda_a$. Moreover, we observed that the omni-directional sensing technique consumes more energy for sensing than the directional sensing technique. This is because, in the omni-directional sensing technique, the sensing range is smaller than

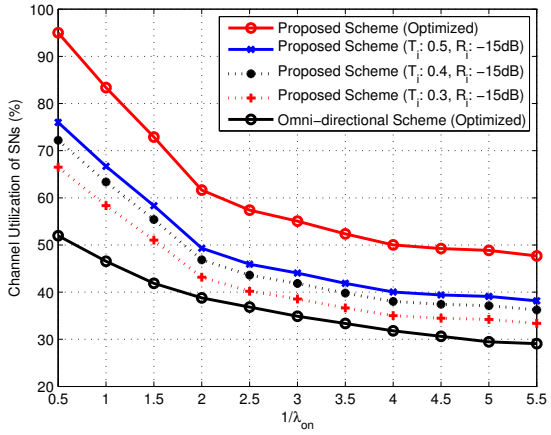

Fig. 12. Channel utilization vs. $1/\lambda_{on}$.

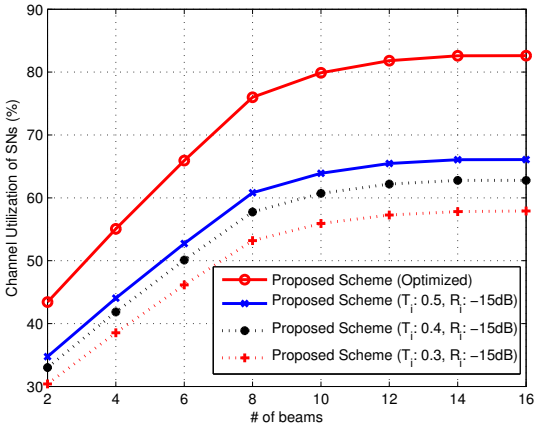

Fig. 14. Channel utilization vs. the number of beams.

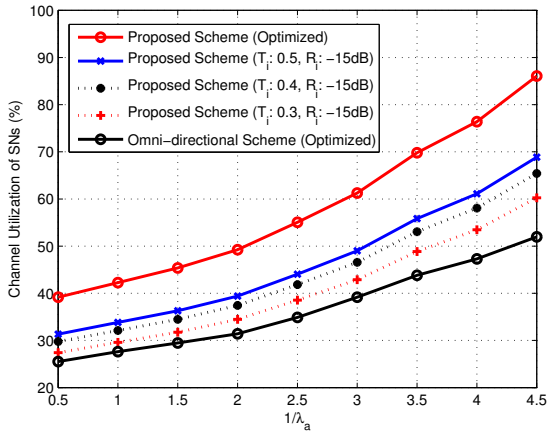

Fig. 13. Channel utilization vs. $1/\lambda_a$.

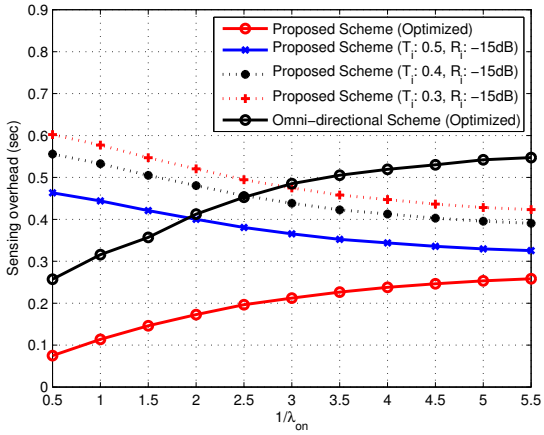

Fig. 15. Unused opportunity vs. $1/\lambda_{on}$.

for the directional sensing scheme. As a result, the cooperative sensing is limited among secondary nodes, which perform more spectrum sensing.

In Fig. 11, the energy consumption increases as M increases. This is because more beams require additional sensing tasks. One interesting finding is that the energy consumption slowly increases after $M = 10$ in the optimization scheme. In the optimized scheme, the FC optimizes the sensing beams and thus energy consumption is almost the same. However, in a non-optimized scheme, the energy consumption still increases after $M = 10$. This is because SN_i uses all beams for spectrum sensing, which causes unnecessary spectrum sensing, such as duplicated sensing. As a result, energy consumption is greater than for the optimized scheme.

Figs. 12, 13, and 14 show the channel utilization versus $1/\lambda_{on}$, $1/\lambda_a$, and the number of beams, respectively. We observe that the channel utilization decreases as $1/\lambda_{on}$ increases, as the time occupied by PUs is longer since SN_i cannot transmit data frames because at least one PU is present. Similarly, the channel utilization increases as $1/\lambda_a$ increases as shown in Fig. 7. Furthermore, in Fig. 14, the channel utilization increases as the number of beams increases, where the narrower beams stimulate spatial reuse.

Fig. 15 shows the sensing overhead versus $1/\lambda_{on}$. Some sensing overheads such as O_f, O_c, and O_u increase at large values of $1/\lambda_{on}$. Additionally, in the non-optimized scheme, the PU detection probabilities are fixed for the entire $1/\lambda_{on}$. As a result, as shown in the figure, the sensing overhead of non-optimized schemes decreases as $1/\lambda_{on}$ increases. On the other hand, the sensing overhead of an optimized schemes (omni-directional sensing and directional sensing) increases as $1/\lambda_{on}$ on increases. This is because T_i becomes shorter than $1/\lambda_{on}$ on to avoid interfering with the PUs occupation of the spectrum channel in the optimized scheme (i.e., it causes more spectrum sensing).

VII. Conclusion

Recently, cognitive radio has been used to solve the problems of spectrum scarcity and usage inefficiency. One of the key techniques of cognitive radio is spectrum sensing, where secondary nodes can detect chunks of unused licensed spectrum. Most of the previous spectrum sensing techniques used an omni-directional antenna. However, the use of directional antennas for spectrum sensing is a promising technique for the realizing a longer sensing range and fine-grained sensing of the PU. In this paper, we propose a directional sensing technique for cognitive radio networks. We assume that one coordinator who is aware of all network information gathers the sensing results from secondary nodes. Using reported information, the coordinator optimizes the length of the sensing period, PU detection margin, channel to sense, and beams to sense per secondary node and assigns the sensing parameters to each secondary node. For optimization, we use a nonlinear optimization technique. The simulation results show that our directional spectrum sensing technique is well suited to the existing cognitive radio environment. In this paper, it is assumed that PU performs omnidirectional communication.

However, in the near future, there will be more PUs that perform communication only in one directional beam. Since the transmission signal of the PU is transmitted in one direction, rather than all directions, it is difficult for the SU to accurately grasp the position of the PU. Additionally, false alarms due to the side lobes of the PU occur frequently. We need to solve this issue, which is our future research problem.

REFERENCES

[1] "ISO/IEC/IEEE International Standard – Information technology – Telecommunications and information exchange between systems – Local and metropolitan area networks– Specific requirements – Part 22: Cognitive Wireless RAN Medium Access Control (MAC) and Physical Layer (PHY) specifications: Policies and procedures for operation in the TV Band," in *ISO/IEC/IEEE* 8802-22:2015 , vol., no., pp.1-678, May 1 2015 doi: 10.1109/IEEESTD.2015.7098301

[2] A. A. Abdullah, L. Cai, and F. Gebali, "DSDMAC: Dual Sensing Directional MAC Protocol for Ad Hoc Networks with Directional Antennas," *IEEE Transactions on Vehicular Technology*, vol. 61, no. 3, 2012.

[3] I. F. Akyildiz, W. Y. Lee, and K. R. Chowdhury, "CRAHNs: Cognitive Radio Ad Hoc Networks," *Ad Hoc Networks*, vol. 7, No. 5, 2009.

[4] I. F. Akyildiz, B. F. Lo, and R. Balakrishnan, "Cooperative Spectrum Sensing in Cognitive Radio Networks: A Survey," *Physical Communication*, no. 4, pp. 40-62, 2011.

[5] S. A. Alvi, M. S. Younis, M. Imran, and F. E. Amin, "A Weighted Linear Combining Scheme for Cooperative Spectrum Sensing," *Precedia Computer Science*, vol. 32, pp. 149-157, 2014

[6] J. Ash and L. Potter, "Sensor Network Localization via Received Signal Strength Measurements with Directional Antennas," *in Proc. of Allerton Conference on Communication, Control, and Computing*, pp. 1861-1870, 2004.

[7] A. Azarfar, J. F. Frigon, and B. Sanso, "Improving the Reliability of Wireless Networks Using Cognitive Radios," *IEEE Communications Survey & Tutorials*, vol. 14, no.2, 2012.

[8] A. Balieiro, P. Yoshioka, K. Dias, D. Cavalcanti, and C. Cordeiro, "A Multi-objective Genetic Optimization for Spectrum Sensing in Cognitive Radio," *Expert Systems with Applications*, vol. 41, no. 8, pp. 3640-3650, 2014.

[9] A. Balieiro, P. Yoshioka, K. Dias, C. Cordeiro, and D. Cavalcanti, "Adaptive spectrum sensing for cognitive radio based on multi-objective genetic optimisation," *Electronics Letters,* vol. 49, no. 17, pp. 1099-1101, 2013.

[10] D. Bera, S. Maheshwari, I. Chakrabarti, and S. S. Pathak, "Decentralized Cooperative Spectrum Sensing in Cognitive Radio Without Fusion Centre," *in Proc. of IEEE NCC*, pp. 1-5, 2014.

[11] A. Bhowmick, M. K. Das, J. Biswas, S. D. Roy, and S. kundu, "Throughput Optimization with Cooperative Spectrum Sensing in Cognitive Radio Network," *in Proc. of IEEE IACC*, pp. 329-332, 2014.

[12] K. Bian, J. M. Park, and B. Gao, "Coexistence-Aware Spectrum Sharing for Homogeneous Cognitve Radio Networks," *Cognitive Radio Networks*, pp. 61-75, 2014.

[13] B. F. Lo and I. F. Akildiz, "Reinforcement Learning for Cooperative Sensing Gain in Cognitive Radio Ad Hoc Networks," *in Proc. of IEEE PIMRC*, pp. 2244-2249, 2010.

[14] P. Cheng, R. Deng, and J. Chen, "Energy-efficient Cooperative Spectrum Sensing in Sensor-aided Cognitive Radio Networks," *IEEE Wireless Communications*, vol. 19, no. 6, pp. 100-105, 2012.

[15] F. F. Digham, M. S. Alouini, and M. K. Simon, "On the Energy Detection of Unknown Signals over Fading Channels," *IEEE transactions on communications*, vol. 55, no. 1, pp. 21-24, 2007

[16] A. Forsgren, P. Gill, M. Wright, "Interior Methods for Nonlinear Optimization", *SIAM review*, vol. 44, no. 4, pp. 525-597, 2002

[17] H. Kim and K. G. Shin. "Efficient Discovery of Spectrum Opportunities with MAC-layer Sensing in Cognitive Radio Networks." *IEEE Transactions on Mobile Computing*, vol. 7, no. 5, pp. 533-545, 2008.

[18] E. Kranakis, D. Krizanc, and E. Williams, "Directional versus omnidirectional antennas for energy consumption and k-connectivity of networks of sensors," *International Conference On Principles Of Distributed Systems*, pp. 357-368, 2004.

[19] H. Li, X. Cheng, K. Li, X. Xing, and T. Jing, "Utility-Based Cooperative Spectrum Sensing Scheduling in Cognitive Radio Networks," *in Proc. of IEEE INFOCOM*, pp. 165-169, 2013.

[20] Y. Li and K. Luk, "60-GHz dual-polarized two-dimensional switch-beam wideband antenna array of magneto-electric dipoles ," *in Proc. of IEEE ISAP*, pp. 1542-1543, 2015.

[21] J. Li and J. Xie, "Directional Antenna Based Distributed Blind Rendezvous in Cognitive Radio Ad-Hoc Networks," *in Proc. of IEEE GLOBECOM,* 2015.

[22] D. Wu, Y. Fan, M. Zhao, and Y. H. Zhang, "Millimeter wave omnidirectional quasi-Yagi array," *Progress In Electromagnetics Research Letters*, vol. 5, pp. 123-130, 2008.

[23] C. Liu and M. Jin, "Maximum-Minimum Spatial Spectrum Detection for Cognitive Radio using Parasitic Antenna Arrays," *in Proc. of IEEE Symposium on Signal Processing for Communications*, pp. 365-369, 2-14.

[24] N. Malhotra, M. Krasniewski, C. Yang, S. Bagchi and W. Chappell, "Location Estimation in Ad Hoc Networks with Directional Antennas," *in Proc. of IEEE International Conference on Distributed Computing Systems*, pp. 633-642, 2005.

[25] N. Murtaza, R. K. Sharma, R. S. Thoma, and M. A. Hein, "Directional Antennas for Cognitive Radio: Analysis and Design Recommendations," *Progress In Electromagnetics Research,* Vol. 140, 2013.

[26] W. Na, L. Park, and S. Cho, "Deafness-aware MAC Protocol for Directional Antennas in Wireless Ad Hoc Networks," *Elsevier Ad Hoc Networks Journal*, vol. 24, Part A, pp. 121-134, 2015 .

[27] N. Noorshams, M. Malboubi, and A. Bahai, "Centralized and Decentralized Cooperative Spectrum Sensing in Cognitive Radio Networks: A Novel Approach," *in Proc. of SPAWC*, pp. 1-5, 2010.

[28] L. Park, C. Lee, and S. Cho, "SPARM: Spatially Pipelined ACK Aggregation for Reliable Multicast in Directional MAC," *IEEE Communication Letters*, vol. 17, no. 3, 2013.

[29] J. Qiao, L.X. Cai, X. Shen, "Multi-Hop Concurrent Transmission in Millimeter Wave WPANs with Directional Antenna," *in Proc. of IEEE ICC*, pp. 1-5, 2010.

[30] B. H. Qureshi, R. K. Sharma, and R. S. Thoma, " Joint spectrum sensing and transmission using a sector antenna in cognitive radio network," *in Proc. of IEEE EuCAP*, pp. 2536-2540, 2014.

[31] W. Si, A.Y. Zomaya,and S. Selvakennedy, "A Geometric Deployment and Routing Scheme for Directional Wireless Mesh Networks," *IEEE Transactions on Computers*, pp. 1323-1335, vol. 63, 2014.

[32] C. Song and Q. Zhang, "Cooperative Spectrum Sensing with Multi-channel Coordination in Cognitive Radio Networks," *in Proc. of IEEE ICC*, pp. 23-27, 2010.

[33] H. Su and S. Moh, "A Directional Cognitive-Radio-Aware MAC Protocol for Cognitive Radio Sensor Networks," *International Journal of Smart Home*, 9(4), 2015.

[34] D. Treeumnuk, S. L. Macdonald, and D. C. Popescu, "Optimizing Performance of Cooperative Sensing for Increased Spectrum Utilization in Dynamic Cognitive Radio Systems," *in Proc. of IEEE ICC*, 2013.

[35] P. Tseng and S. Yun, "Block-coordinate gradient descent method for linearly constrained nonsmooth separable optimization", *Journal of optimization theory and applications*, vol. 140, no. 3, pp. 513-535, 2009

[36] J. Unnikrishnan and V.V. Veeravalli, " Cooperative Sensing for Primary Detection in Cognitive Radio," *IEEE Journal of Selected Topics in Signal Processing*, no. 2, pp. 18-27, 2008.

[37] B. Wang, K. J. Jay, and T. C. Clancy, "Evolutionary Cooperative Spectrum Sensing Game: How to Collaborate?," *IEEE Transactions on Communications*, vol. 58, no. 3, 2010.

[38] D. L. Wasden, H. Moradi, and B. Farhang-Boroujeny, "Design and Implementation of an Underlay Control Channel for Cognitive Radios," *IEEE Journal on Selected Areas in Communications*, vol. 30, no. 10, 2012

[39] D. Wilcox, E. Tsakalaki, A. Kortun, T. Ratnarajah, and C. B. Papadias, and M. Sellathurai, "On Spatial Domain Cognitive Radio Using Single-Radio Parasitic Antenna Arrays," *IEEE Journal on Selected Area in Communications*, vol. 31, no. 3, 2013.

[40] L. Yang, S. H. Song, and K. B. Letaief "Optimizing Spectrum Sensing Efficiency in Cognitive Radio Networks," *in Proc. of ComComAp*, pp. 262-266, 2012.

[41] Y. Yuan, "A review of trust region algorithms for optimization", *in Proc. of ICIAM*, vol. 99, pp. 271–282, 2000

[42] T. Zhang, R. Safavi, and Z. Li, "ReDiSen: Reputation-based Secure Cooperative Sensing in Distributed Cognitive Radio Networks," *in Proc. of IEEE ICC*, pp.2601-2605, 2013.

[43] Y. Zhao, J. Huang, W. Wang, and R. Zaman, "Detection of Primary User's Signal in Cognitive Radio Networks: Angle of Arrival based Approach," *in Proc. of IEEE Globecom*, pp.3062-3067, 2014.

[44] Y. Zheng, X. Xie, and L. Yang, "Cooperative Spectrum Sensing Based on SNR Comparison in Fusion Center for Cognitive Radio," *in Proc. of IEEE ICACC*, pp. 212-216, 2009.

[45] F. Zeng, C. Li, and Z. Tian, "Distributed Compressive Spectrum Sensing in Cooperative Multihop Cognitive Networks," *IEEE Journal of Selected Topics in Signal Processing*, vol. 5, no. 1, 2011.

[46] Z. Luo, W. Yu, "An Introduction to Convex Optimization for Communications and Signal Processing," *IEEE Journal of Selected Areas in Communications*, vol. 24, no. 8, pp. 1426-1438, 2006.

Woongsoo Na received his B.S., M.S., and Ph.D. degrees in Computer Science and Engineering from Chung-Ang University, Seoul, Korea in 2010, 2012, and 2017, respectively. He is currently a adjunct professor in the School of Infomation Technology at Sungshin University, Seoul, Korea. His research interests include mobile chargers, directional MAC, wireless mobile networks, and LTE.

Jongha Yoon received B.S. and M.S degrees in Computer Science and Engineering from Chung-Ang University, Seoul, Korea in 2014 and 2016, respectively. He is currently an instructor in Department of Electronics and Communications Engineering, Republic of Korea Air Force Academy, Cheongju, Republic of Korea since 2016. His research interests include Cognitive Radio, Tactical Data Link, and Directional MAC.

Sungrae Cho received his Ph.D. degree in electrical and computer engineering from Georgia Institute of Technology, Atlanta, Georgia, USA, in 2002, and his B.S. and M.S. degrees in electronics engineering from Korea University, Seoul, Korea, in 1992 and 1994, respectively. He is currently a full professor with the School of Computer Science and Engineering, Chung-Ang University, Seoul, Korea. Prior to joining Chung-Ang University, he was an assistant professor with the Department of Computer Sciences, Georgia Southern University, Statesboro, Georgia, USA, from 2003 to 2006, and a Senior Member of Technical Staff with Samsung Advanced Institute of Technology (SAIT), Kiheung, Korea, in 2003. From 1994 to 1996, he was a Member of Research Staff with the Electronics and Telecommunications Research Institute (ETRI), Daejeon, Korea. From 2012 to 2013, he held a Visiting Professorship with the National Institute of Standards and Technology (NIST), Gaithersburg, Maryland, USA. He is an Editor of the Elsevier Ad Hoc Networks Journal since 2012 and has served numerous international conferences as an organizing committee member, such as IEEE SECON, ICOIN, ICTC, ICUFN, TridentCom, and IEEE MASS. His research interests include wireless networking, ubiquitous computing, performance evaluation, and queuing theory.

Nada Golmie received her Ph.D. in computer science from the University of Maryland at College Park. Since 1993, she has been a research engineer at the National Institute of Standards and Technology (NIST). She is currently the chief of the wireless networks division in the Communications Technology Laboratory. Her research in media access control and protocols for wireless networks led to over 100 technical papers presented at professional conferences, journals, and contributed to international standard organizations and industry led consortia. She is the author of "Coexistence in Wireless Networks: Challenges and System-level Solutions in the Unlicensed Bands," published by Cambridge University Press (2006).

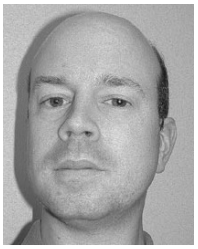

David Griffith received the B.E.E. (cum laude), M.E.E., and Ph.D. degrees from the University of Delaware, Newark, in 1990, 1994, and 1997, respectively. From 1990 to 1992, he was a Systems Engineer with Stanford Telecommunications, Reston, VA. From 1997 to 1999, he worked with the Command, Control, and Communications Division, Raytheon Systems Company, Marlborough, MA. In December of 1999, he joined the High-Speed Networking Group, National Institute of Standards and Technology (NIST), Gaithersburg, MD. His research interests include GMPLS control plane design and protection and restoration algorithms for robust optical networks. Dr. Griffith is involved with the Internet Engineering Task Force (IETF) and the Optical Internetworking Forum (OIF). He is a Member of the IEEE Communications Society, the SPIE Optical Networks Technical Group, and the Tau Beta Pi, Eta Kappa Nu, and Phi Kappa Phi honor societies. He is co-editor of the Standards Section of SPIEs Optical Networks Magazine.